Effect of long-range interactions on the critical behavior of the continuous Ising model

E. Bayong and H. T. Diep*
Laboratoire de Physique Théorique et Modélisation, Université de Cergy-Pontoise, 2 Avenue Adolphe Chauvin, 95302 Cergy-Pontoise Cedex, France
(Received 1 December 1998)

Critical behavior of the one- and two-dimensional general continuous Ising models with long-range ferromagnetic interactions decaying as $1/r^{d+\sigma}$ is studied using a histogram Monte Carlo technique. A continuous Ising model means that a spin can take any value between -1 and 1. It is found that the system exhibits a second-order phase transition with nonstandard critical exponents which depend on σ. Results for various values of σ will be shown and compared to predictions from renormalization-group theory. Though there is an agreement with the overall tendency predicted, there are several fundamental differences. Discussion is given. [S0163-1829(99)02718-6]

I. INTRODUCTION

In statistical mechanics, most models are limited to nearest-neighbor (NN) interactions. Many properties of such models are known with precision. In particular, critical behaviors can be either exactly derived[1] or precisely obtained in certain limits. One can mention the solution of Onsager[2] for the two-dimensional (2D) Ising model, the vertex solvable models,[1] the critical exponents for various spin models in 2 and 3D.[3–5] It is known, however, that when long-range (LR) interactions are included, the situation often becomes complicated. For instance, when next-nearest-neighbor (NNN) interactions compete with the (NN) one, the system becomes frustrated. Though much interesting physics has recently been discovered for such systems,[6] well-established theoretical methods often fail to predict correct behaviors.

We are interested here in the effect of LR interactions decaying with distance r as $1/r^{d+\sigma}$, in 1 and 2D. It is known that LR forces can induce critical behavior in 1D systems where it would otherwise be absent. There have been some analytical studies as well as a number of numerical results on critical behavior of these systems. The 1D Ising model with algebraically decaying LR interactions have been extensively investigated during the last two decades. It is known that it exhibits LR order at finite temperature (T) if $\sigma \leqslant 1$ and no phase transition if $\sigma > 1$.[7–12] The detailed properties of the spherical model with LR interactions have been discussed by Joyce.[13] It is noted, however, that there is no rigorous information about the critical exponents of such systems. Fisher *et al.* have studied the critical exponents on a general system with n-component order parameter[14] using a renormalization-group (RG) method. These exponents depend on the values of n, σ, and d. For $\sigma > 2$, they take the values of short-range (SR) exponents for all d. A RG expansion in $1-\sigma > 0$ has been done by Kosterlitz[15] who obtained $1/\nu = [2(1-\sigma)^{1/2}]$ when $\sigma \to 1$ in 1D. In the case of the Ising model, the critical temperature T_c and critical exponents have been evaluated by Glumac and Uzelac[10,11] using the transfer matrix with a finite-range scaling. This evaluation has been also made by finite chain extrapolations.[16] Note that a 1D spin-glass Ising model with LR algebraically decaying interactions has been investigated by Kotliar *et al.*[17]

These examples show that while the Ising case has been widely investigated, non-Ising models have not received much attention. Recently, Glumac and Uzelac[20] have investigated the 1D q-state Potts model up to $q = 64$ using a transfer-matrix method with a cutoff at 20 atomic distances. Priest and Lubensky[18] and Thumann and Gusmao[19] have used a RG expansion in $\epsilon = 3\sigma - d$ to calculate critical exponents of the Potts model. Note that in the case of LR d-dimensional systems, except the early work for $d = 1$ with very small sizes (up to 15 spins),[8] Monte Carlo (MC) techniques have not been used. This is partially due to the long computing time required. The absence of reliable MC results, in particular in the non-Ising case, has motivated the present work.

In this paper we present simulation results for the 1- and 2D continuous Ising models using standard MC simulations and the MC histogram method. Our purpose is to compare our MC results with the predictions of RG calculations.[14,15,7]

In Sec. II we present the results obtained for 1 and 2D with varying σ. The values of different critical exponents are shown and compared to RG predictions. One of our striking results is the absence of a first-order transition unlike the case of SR standard Potts model with a large q in 2 and 3D. Concluding remarks are given in Sec. III.

II. RESULTS OF MONTE CARLO SIMULATIONS

The continuous Ising model in dimension d that we shall consider is defined as

$$\mathcal{H} = -\sum_{\langle i,j \rangle} J_{ij}\sigma_i\sigma_j , \tag{1}$$

where σ_i is a classical Ising spin at site i and takes all values between -1 and 1, and $J_{ij} = 1/|i-j|^{d+\sigma}$. We take into account all interactions without cutoff permitted by the periodic boundary conditions, i.e., $|i-j| < L/2$ where L is the linear system size. In 1D, we simulated systems with linear sizes in the range $L = 50-900$. In 2D, we used samples sizes up to $L \times L = 36^2$. A MC step per site (MCS/site) for a LR

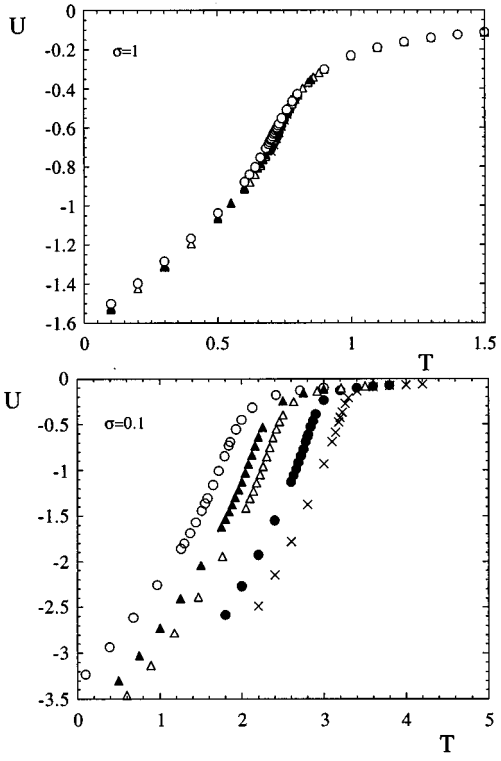

FIG. 1. Temperature and size dependences of internal energy U for $\sigma=1$ (upper) and $\sigma=0.1$ (lower). Void circles, black triangles, white triangles, black circles, and crosses are for $L=50$, 100, 150, 400, and 900, respectively.

Ising model involves $O(L^2)$ or $O(L^4)$ operations in 1- or 2D. The system size is thus limited in order to spend a reasonable computing time due the presence of LR interactions. The simulations of the model were carried out for many values of σ.

We use first the standard MC simulations: the equilibrating time is from 100 000 to 200 000 MCS/spin and the averaging time is from 500 000 to 1 000 000 MCS/spin. We use the results of standard MC simulations to localize for each size the transition temperature $T_c(L)$ where histogram measures are performed. For histogram measures, we discard 1 million MCS/spin and measure between 3 and 5 million MCS/spin. The histograms[21] are then used to determine critical exponents. Contrary to the traditional MC calculations, we do not need a previous knowledge of T_c with high precision. The following quantities have been calculated: magnetization M, total energy E, specific heat C_v, susceptibility χ, first-order cumulant of the energy C_U, nth-order cumulant of the order parameter V_n for $n=1$ and 2:

$$\langle M\rangle=\left\langle \sum_i \sigma_i \right\rangle, \tag{2}$$

$$\langle E\rangle=\langle \mathcal{H}\rangle, \tag{3}$$

$$C_v=\frac{1}{k_B T^2}(\langle E^2\rangle-\langle E\rangle^2), \tag{4}$$

TABLE I. The 1D case. The transition temperatures $T_c(L)$ associated with the peak position of C_v for all σ studied in the 1D case.

σ \ L	50	100	150	400	900
0.1	1.75	2.12	2.35	2.81	3.18
0.3	1.35	1.48	1.58	1.80	2.05
0.5	1.10	1.20	1.25	1.35	1.425
0.7	0.94	0.95	0.96	1.02	1.06
1	0.71	0.71	0.71	0.71	0.71
1.1	0.66	0.66	0.66	0.66	0.66

$$\chi=\frac{1}{k_B T}(\langle M^2\rangle-\langle M\rangle^2), \tag{5}$$

$$C_U=1-\left(\frac{\langle E^4\rangle}{3\langle E^2\rangle^2}\right), \tag{6}$$

$$V_n=\left\langle\left(\frac{\partial \ln M^n}{\partial(1/k_B T)}\right)\right\rangle=\left(\frac{\langle M^n E\rangle}{\langle M^n\rangle}\right)-\langle E\rangle. \tag{7}$$

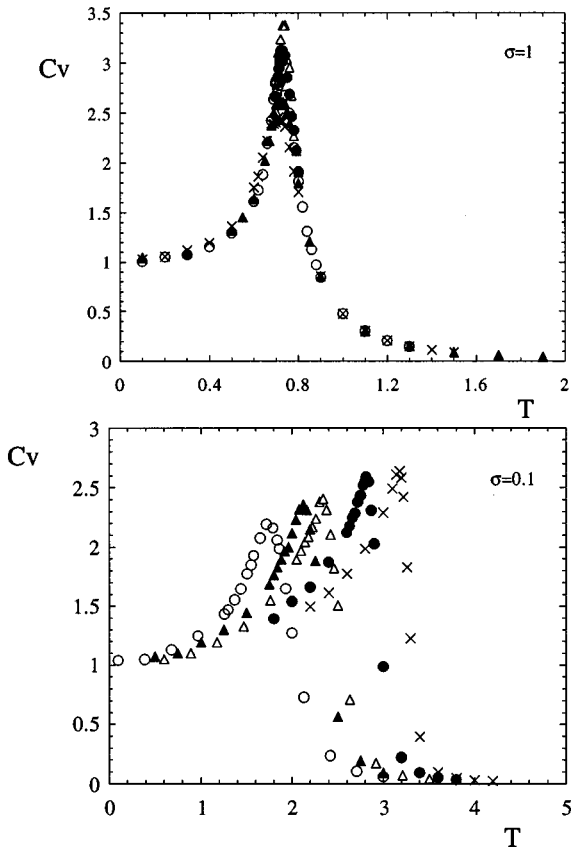

FIG. 2. Temperature and size dependences of the specific heat for $\sigma=1$ (upper) and $\sigma=0.1$ (lower). Void circles, black triangles, white triangles, black circles, and crosses are for $L=50$, 100, 150, 400, and 900, respectively.

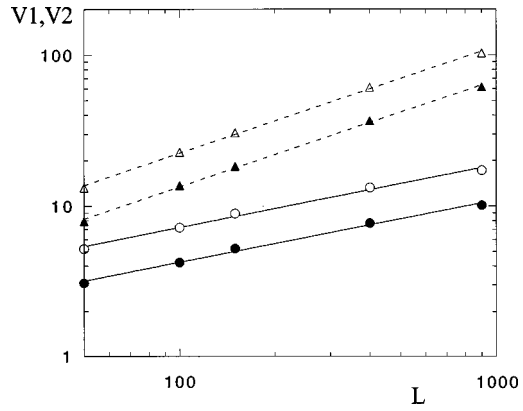

FIG. 3. Determination of the critical exponent ν for $\sigma=0.1$ (triangles) and $\sigma=1$ (circles) from the slope of $V_1^{\min}$ (black) and $V_2^{\min}$ (white) vs L in the ln-ln scale. Errors are smaller than the size of data points.

The mean values may be calculated as continuous functions of temperature using the histogram $H(E)$ obtained at $T_c(L)$ to calculate the canonical probabilities at temperatures T around $T_c(L)$ by

$$P(E,T)=\frac{H(E)\exp[-\Delta\beta E]}{\sum_E H(E)\exp[-\Delta\beta E]}, \tag{8}$$

where $\Delta\beta=1/k_BT_c(L)-1/k_BT$. The thermal average of a physical quantity A is then calculated by

$$\langle A\rangle=\sum_E AP(E,T). \tag{9}$$

The thermal averages are thus calculated as continuous functions of T.

For large values of L, physical quantities are expected to scale with L as follows:

$$V_1^{\min}\propto L^{-1/\nu}, \quad V_2^{\min}\propto L^{-1/\nu}, \tag{10}$$

$$C_U=C_U[T_c(\infty)]+AL^{-\alpha/\nu}, \tag{11}$$

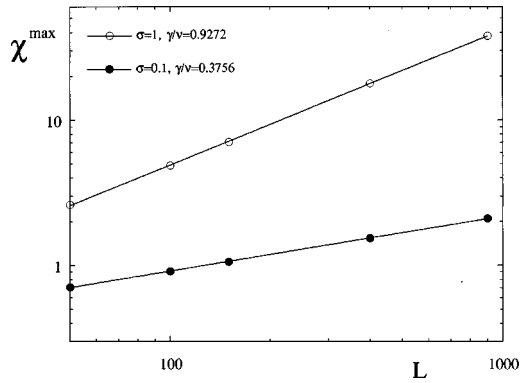

FIG. 4. Determination of the critical exponent γ from the slope of $\chi_{\max}$ vs L in ln-ln scale for $\sigma=0.1$ (black circles) and $\sigma=1$ (void circles). Errors are smaller than the size of data points.

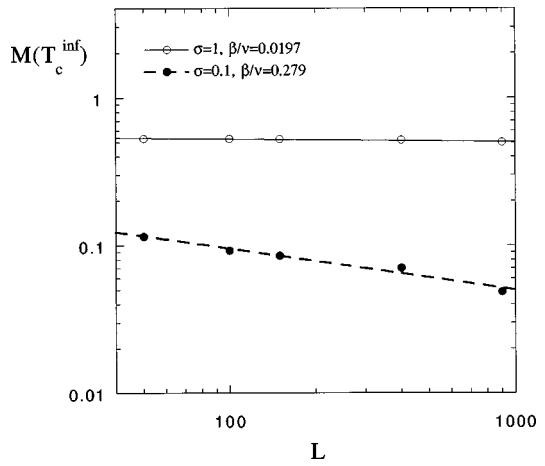

FIG. 5. Determination of β from the slope of $M[T_\infty]$ vs L in ln-ln scale for $\sigma=0.1$ (black circles) and $\sigma=1$ (void circles). Errors are smaller than the size of data points.

$$M_{T_c(\infty)}\propto L^{-\beta/\nu}, \tag{12}$$

$$C_v^{\max}=C_0+C_1L^{\alpha/\nu}, \tag{13}$$

$$\chi^{\max}\propto L^{\gamma/\nu}, \tag{14}$$

and

$$T_c(L)=T_c(\infty)+C_AL^{-1/\nu}, \tag{15}$$

where A,C_0,C_1,C_A are constants. We estimated ν independently from $V_1^{\min}$ and $V_2^{\min}$. With these values we calculated γ from $\chi^{\max}$. We estimated $T_c(\infty)$ by using the last expression for each observable. Using this value of $T_c(\infty)$, we calculated β from $M_{T_c(\infty)}$. The Rushbrooke scaling law $\alpha+2\beta+\gamma=2$ allows us to obtain α. Finally, using the hyperscaling relationship, we can estimate the effective dimension of this model $d_{\text{eff}}=(2-\alpha)\nu^{-1}$ and the exponent η from the scaling law $\gamma=(2-\eta)\nu$.

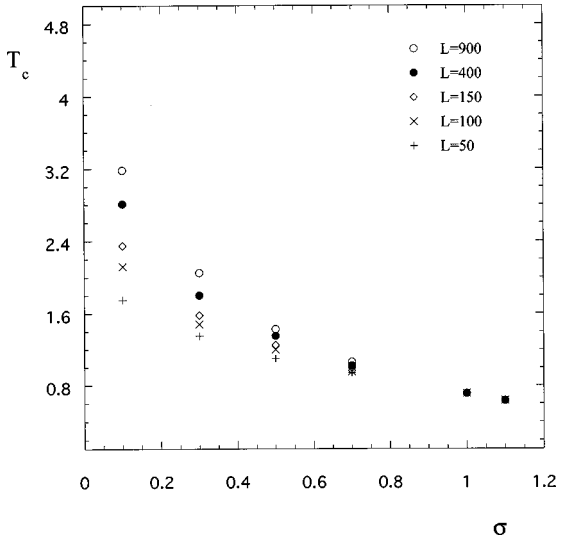

FIG. 6. T_c at different L versus σ. See text for comments.

TABLE II. The 1D case. Critical exponents from the MC histogram method (see text for comments).

σ	ν	γ	β	α	η	d_{eff}	T_c
0.1	1.41(1)	0.53(1)	0.39(1)	0.69(1)	1.62(1)	0.93(1)	3.30(2)
			0.44(1)	0.59(1)			
0.3	1.62(1)	0.73(1)	0.35(1)	0.52(1)	1.55(1)	0.93(1)	2.11(2)
			0.43(1)	0.41(1)			
0.5	1.72(1)	0.99(1)	0.34(1)	0.34(1)	1.43(1)	0.96(1)	1.49(1)
			0.37(1)	0.28(1)			
0.7	1.79(1)	1.26(1)	0.29(1)	0.16(1)	1.30(1)	1.03(1)	1.08(1)
			0.26(1)	0.21(1)			
1	2.42(1)	2.26(1)	0.084(1)	$-0.34(1)$	1.08(1)	0.97(1)	0.72(2)
			0.077(1)	$-0.41(1)$			
1.1	2.80(1)	2.82(1)			0.99(1)		0.63(1)
			0.011(2)	$-0.80(1)$			

A. The 1D case

The values of σ were chosen in the nonclassical regime $0.5<\sigma\leqslant 1$ where critical exponents are expected to depend not only on σ but also on n and d as well as in the case of classical regime $(0<\sigma<0.5)$.[14] In addition, we have also made calculations for $\sigma>1$ to see if there exists a phase transition at finite T for the continuous Ising model studied here since it has been shown[7] in the Ising case that there is no transition at finite T for $\sigma>1$.

We performed first the standard MC simulations where the magnetization per site m, energy per site U, specific heat C_v, and susceptibility χ were measured as functions of the temperature T. The results of U versus T present a single inflection point suggesting the occurence of a continuous transition. Examples are shown in Fig. 1 with several lattice sizes for $\sigma=0.1$ and 1. For $\sigma=1$ a very small size dependence is observed, while smaller values of σ have very strong size dependence. Table I shows the critical temperature $T_c(L)$ for several values of σ. In Fig. 2, we show C_v calculated from energy fluctuations as a function of T for $\sigma=0.1$ and 1, each with several lattice sizes.

We next performed MC histogram calculations for $L=50,100,150,400,900$. Between 3 and 5 million MCS/site were performed for each lattice size. The results show that the transition is clearly of second order. The asymptotic value of C_U tends to 2/3 for large L (not shown). Figure 3 presents the minima of V_1 and V_2 as functions of L in the ln-ln scale. The data lie nicely on a straight line whose slope is $1/\nu$. We obtain $\nu=1.41(1)$ and $\nu=2.42(1)$ for $\sigma=0.1$ and 1, respectively. The errors were estimated from the line-fitting procedure. Systematic errors from estimates of $T_c(L)$ were much smaller. The maximum of χ versus L is shown in Fig. 4 for $\sigma=0.1,1$. The slope of each line yields the value of γ/ν. Using the values of ν one obtains γ. Now, with the values of Table I we obtain by scaling $T_c(\infty)$. Plotting $M_{T_c(\infty)}$ versus $L^{-\beta/\nu}$ in the ln-ln scale, one obtains directly β/ν. Examples are shown in Fig. 5. Using the Rushbrooke relationship, one obtains α. The scaling relationship then gives the effective dimensionality d_{eff}. Criticals exponents are resumed in Table II where the values in the second lines of β and α are those obtained by using first $\alpha=2-d\nu$ with $d=1$ and then calculating β with $\beta=(2-\gamma-\alpha)/2$. Though the orders of magnitude and the sign of these deduced values are in a qualitative agreement with those in the first lines, we think, however, that the latter values are more reliable due to the fact that only one scaling relation is used.

Several remarks are in order:

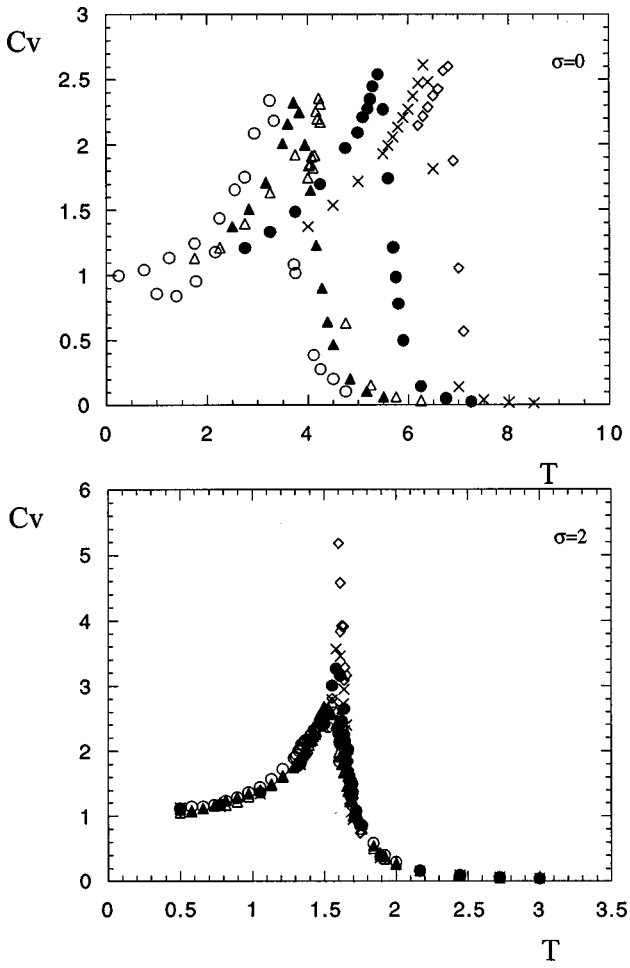

FIG. 7. The 2D case. Temperature and size dependences of the specific heat for two extreme cases $\sigma=0$ (upper) and $\sigma=2$ (lower) $\sigma=0$. Void circles, black triangles, white triangles, black circles, crosses, and diamonds are for $L=8$, 10, 12, 20, 30, and 36, respectively.

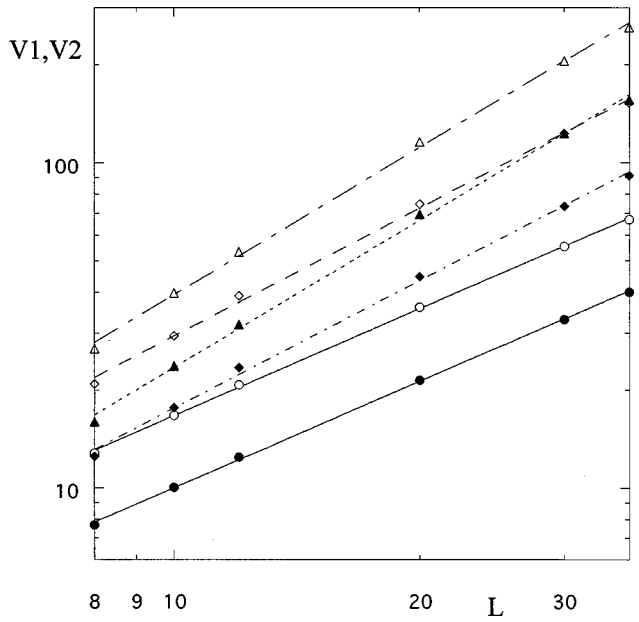

FIG. 8. The 2D case. Determination of the critical exponent ν for $\sigma=2$ (circles), $\sigma=0.5$ (diamonds), and $\sigma=0$ (triangles) from the slope of $V_1^{\min}$ (black) and $V_2^{\min}$ (white) vs L in ln-ln scale. Errors are smaller than the size of data points.

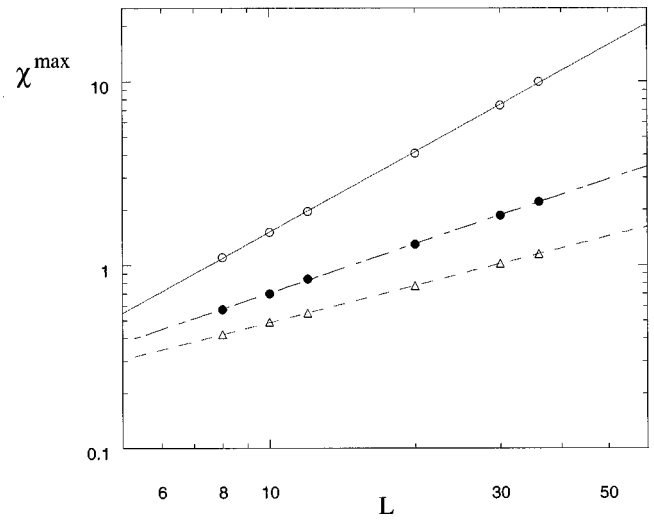

FIG. 9. The 2D case. Determination of the critical exponent γ from the slope (γ/ν) of $\chi^{\max}$ vs L in ln-ln scale for $\sigma=2$ (white circles), 0.5 (black circles), and 0 (triangles). Errors are smaller than the size of data points.

(i) The very small size dependence when $\sigma \geqslant 1$ explains the large value of ν.

(ii) We do not however find the divergence of ν when $\sigma=1$ as it was predicted for the 1D Ising case.[15]

(iii) Thouless[7] has showed that in the Ising case with $\sigma=1$ the transition is either of first order or $\beta=0$. Our result shows that the transition is of second order with $\beta=0.084(1)$ for the continuous Ising spins studied here. In addition, for $\sigma=1.1$ on still has the transition at finite T (see Fig. 6), contrary to the discrete Ising case. Note, however, that we have made calculations for $\sigma=2$ and we did not find a finite-T transition. There may thus be a difference between discrete and continuous Ising models.

(iv) Our results for ν are far from those obtained by Glumac and Uzelac[20] for the standard Potts model: for $q=64$ they obtained $\nu=1$ where $\sigma=1$, and for $q=16$ they gave $\nu=0.22$ for $\sigma=0.7$. The continuous Ising model shown here is thus different from the standard large-q Potts model.

(v) In the so-called classical regime ($\sigma<0.5$), our results are different from those of Fisher *et al.*[14] Note that γ given by Nagle and Bonner[16] in the Ising case in the classical regime is also different from ours. In the nonclassical regime, our results are in agreement with the values by Fisher *et al.* for η and γ with a very small correction to the expression $\eta=2-\sigma$ (see values of η), and with MC results of Nagle and Bonner for the 1D Ising case.[16]

B. The 2D case

We consider the continuous Ising model on the square lattice. As in the 1D case, we performed first standard MC simultions to locate $T_c(L)$ for each linear lattice size for a given σ. Then, we employed the MC histogram technique to calculate critical exponents.

Note that our MC programs are very efficient: the test for the SR Ising model up to $L=50$ gives the critical exponents within 0.5% of the exact values. Let us add that our results for the continuous Ising model with only nearest-neighbor interactions agree within 1% with the exact values of the SR Ising model.

Now, for the present LR continuous Ising model, we have studied the following values of σ: 0, 0.5, 1, 1.5, 2, and 3, for a systematic comparison. For each value, various L up to 36

TABLE III. The 2D case. Critical exponents from the MC histogram method. For comparison, values for *short-range* Ising, three-state Potts, and continuous Ising models are also displayed. See text for comments.

Systems	Interactions	ν	γ	α	β	η	T_c
Ising (q=2)	SR (exact)	1	1.75	0	0.125	0.25	2.27
Potts (q=3)	SR	0.83(1)	1.46(1)	0.34(1)	0.10(1)	0.23(1)	0.99(1)
Ising (q=infinite)	SR	1.02(1)	1.78(1)	−0.04(1)	0.13(1)	0.25(1)	0.90(1)
	LR ($\sigma=3$)	0.99(1)	1.64(1)	−0.02(1)	0.18(1)	0.35(1)	1.28(1)
	LR ($\sigma=2$)	0.92(1)	1.34(1)	0.16(1)	0.25(1)	0.54(1)	1.65(1)
	LR ($\sigma=1.5$)	0.88(1)	1.13(1)	0.23(1)	0.32(1)	0.73(1)	2.03(1)
	LR ($\sigma=1$)	0.84(1)	0.90(1)	0.32(1)	0.39(1)	0.92(1)	2.75(1)
	LR ($\sigma=0.5$)	0.76(1)	0.68(1)	0.48(1)	0.42(1)	1.12(1)	4.20(1)
	LR ($\sigma=0$)	0.44(1)	0.64(1)	1.12(1)	0.12(1)	1.34(1)	7.74(1)

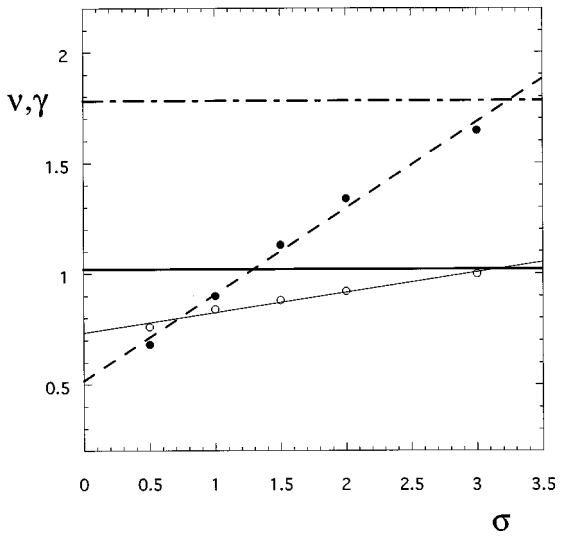

FIG. 10. The 2D case. ν (void circles) and γ (black circles) versus σ. Short-range value of $\nu(\gamma)$ is drawn by horizontal continued (discontinued) line. The values for $\sigma=0$ which are not on the fitted lines are not shown. See text for comment.

are used. We show in Fig. 7 the specific heat as a function of L for two extreme cases $\sigma=2$ and 0, for comparison. As seen, the smaller σ is the stronger the size effect has on $T_c(L)$. Histograms have been taken at $T_c(L)$ at every size for each σ. The ln-ln plot of $V_1^{\min}$ and $V_2^{\min}$ versus L gives ν, and the ln-ln plot of $\chi^{\max}$ versus L yields γ/ν. Examples are shown in Figs. 8 and 9 for $\sigma=2$, 0.5, and 0. Table III shows all calculated critical exponents. Though all exponents have a tendency toward their SR values when σ is increased, we observe that for $\sigma=2$, their values are not yet very close to the values of the SR Ising (and continuous Ising) model. This finding shows that the prediction of Fisher *et al.*[14] for the discrete Ising model, according to which for $\sigma>2$ critical exponents take the SR values, should be modified for the present continuous Ising model. We show in Fig. 10 the values of ν and γ versus γ where the SR values are approached only at $\sigma=3$.

III. CONCLUDING REMARKS

We have studied the general continuous Ising model with LR interactions decaying as a power law of distance, using the MC histogram method and finite-size scaling in one and two dimensions. We found the transition to be continuous with critical exponents obtained systematically for all relevant σ. Though the general aspects of our results are in agreement with the tendency predicted by RG calculations for the Ising model, the details of our continuous Ising model are somewhat different. For instance, in 1D, for the case where $\sigma=1$, our result shows a large value of ν but far from the divergent value predicted for the Ising model.[15] In addition, unlike in the case of the discrete Ising model, our results indicate that there is a phase transition at finite T even for $\sigma=1.1$. The finite T transition disappears at higher σ. In 2D, our critical exponents indicate that they take the SR values only when $\sigma\geqslant 3$, instead of $\sigma>2$ given by the RG calculations for the Ising case.[14] Moreover, in the classical regime our results do not verify RG results. In conclusion, we think that it would be interesting to reconsider previous theories for the case of the continuous Ising model presented in this paper.

ACKNOWLEDGMENT

Laboratoire de Physique Théorique et Modélisation is associated with CNRS (EP 0127).

*Electronic address: Hung-The.Diep@ptm.u-cergy.fr

[1] R. J. Baxter, *Exactly Solved Models in Statistical Mechanics* (Academic, New York, 1992).
[2] L. Onsager, Phys. Rev. **65**, 117 (1944).
[3] See, for example, D. J. Amit, *Field Theory, Renormalization Group and Critical Phenomena* (McGraw-Hill, New York, 1978); S. K. Ma, *Modern Theory of Critical Phenomena* (Benjamin, New York, 1976).
[4] K. G. Wilson, Phys. Rev. B **4**, 3174 (1971); **4**, 3184 (1971).
[5] J. C. Le Guillou and J. Zinn-Justin, J. Phys. (France) Lett. **46**, L137 (1985).
[6] For recent reviews, see *Magnetic Systems with Competing Interactions (Frustrated Spin Systems)*, edited by H. T. Diep (World Scientific, Singapore, 1994).
[7] D. J. Thouless, Phys. Rev. **187**, 732 (1969).
[8] D. Rapaport and N. E. Frankel, Phys. Lett. A **28**, 405 (1968).
[9] See references given, in E. Luitjen and H. W. J. Blote, Phys. Rev. Lett. **76**, 1557 (1996); **76**, 3662 (1996); Phys. Rev. B **56** 8945 (1997).
[10] Z. Glumac and K. Uzelac, J. Phys. A **22**, 4439 (1989).
[11] Z. Glumac and K. Uzelac, J. Phys. A **24**, 501 (1991).
[12] M. J. Wragg and G. A. Gehring, J. Phys. A **23**, L2157 (1990).
[13] G. S. Joyce, Phys. Rev. **146**, 349 (1966).
[14] Michael E. Fisher, Shang-keng Ma, and B. G. Nickel, Phys. Rev. Lett. **29**, 917 (1972).
[15] J. M. Kosterlitz, Phys. Rev. Lett. **37**, 1577 (1976).
[16] J. F. Nagle and J. C. Bonner, J. Phys. C **3**, 352 (1970).
[17] G. Kotliar, P. W. Anderson, and D. L. Stein, Phys. Rev. B **27**, 602 (1983).
[18] R. G. Priest and T. C. Lubensky, Phys. Rev. B **13**, 4159 (1976).
[19] W. K. Theumann and M. A. Gusmao, Phys. Rev. B **31**, 379 (1985).
[20] Z. Glumac and K. Uzelac, J. Phys. A **26**, 5267 (1993).
[21] A. M. Ferrenberg and R. H. Swendsen, Phys. Rev. Lett. **61**, 2635 (1988); Phys. Rev. B **44**, 5081 (1991).